Timely excision of prophage Φ13 is essential for the *Staphylococcus aureus* infectious process

Olivier Poupel,[1] Gérald Kenanian,[1] Lhousseine Touqui,[2] Charlotte Abrial,[2] Tarek Msadek[1,6*], Sarah Dubrac[1,3,6*]

[1] Institut Pasteur, Université Paris Cité, CNRS UMR2001, Department of Microbiology, Biology of Gram-Positive Pathogens Unit, F-75015 Paris, France

[2] Institut Pasteur, Université Paris Cité, Department of Global Health, Cystic Fibrosis and Bronchial Diseases Unit, F-75015 Paris, France.

[3] Present address: Institut Pasteur, Université Paris Cité, CNRS UMR6047, Department of Microbiology, Stress Adaptation and Metabolism in Enterobacteria Unit, F-75015 Paris, France

[6]These authors jointly supervised this work : Tarek Msadek, Sarah Dubrac.

*Address correspondence to Tarek Msadek, tmsadek@pasteur.fr, or Sarah Dubrac sarah.dubrac@pasteur.fr

ABSTRACT Mobile genetic elements play an essential part in the infectious process of major pathogens, yet the role of prophage dynamics in *Staphylococcus aureus* pathogenesis is still not well understood. Here we studied the impact of the Φ13 *hlb*-converting prophage, whose integration inactivates the *hlb* β-toxin gene, on staphylococcal pathogenesis. We showed that prophage Φ13 is lost in approximately half the bacterial population during the course of infection. Inactivation of the Φ13 *int* recombinase gene, essential for insertion/excision, locked the prophage in the bacterial chromosome, leading to a significant loss of virulence in a murine systemic infection model. In contrast, the non-lysogen strain (ΔΦ13), where the *hlb* beta-hemolysin gene is reconstituted, displayed strongly increased virulence. Accordingly, histopathological analyses revealed more severe nephritis in mice infected with bacteria lacking prophage Φ13 (ΔΦ13), compared to infection with the parental strain. Infection with the Δ*int* mutant, where beta-hemolysin production is abolished, led to the least severe renal lesions. Cytokine induction in a human neutrophil model showed significantly increased IL-6 expression following infection with the beta-hemolysin producing strain (ΔΦ13). Our results indicate that timely *in vivo* excision of the Φ13 prophage is essential for progression of the *Staphylococcus aureus* infectious process: early excision leads to rapid host death whereas the inability to excise the prophage significantly reduces staphylococcal virulence.

IMPORTANCE This study highlights prophage Φ13 excision as a critical factor in *S. aureus* pathogenesis, influencing infection outcomes by balancing rapid host killing with reduced bacterial virulence. This mechanism may represent a bet-hedging strategy in genetic regulation, resulting in a mixed bacterial population capable of rapidly switching between two processes: bacterial colonization and host damage. Unraveling this dynamic opens new possibilities for developing targeted therapies to disrupt or modulate prophage activity, offering a novel approach to mitigating *S. aureus* infections.

51 **INTRODUCTION**

52 *Staphylococcus aureus*, a major human pathogen, causes severe invasive infectious
53 diseases targeting every type of organ, such as pneumonia, endocarditis, osteomyelitis
54 or septicemia. Yet it is also a commensal, asymptomatically colonizing up to 30% of
55 the human population, with the transition between the two lifestyles poorly
56 understood (1). Mobile genetic elements make up approximately 20% of its genome,
57 leading to variations in gene combinations that can strongly influence *S. aureus*
58 virulence (2). Among these, temperate bacteriophages play an important role in
59 genetic variability. Φ13, a member of the Sa3int Siphoviridae *S. aureus* bacteriophage
60 family, is responsible for a dual phenotypic conversion (3, 4) and is by far the most
61 widespread among human clinical isolates (5). Its chromosomal attachment site (*attB*)
62 lies within the coding sequence of the hemolysin B gene, *hlb*, encoding the neutral
63 sphingomyelinase C β-toxin, such that it acts as a phage regulatory switch (6). Φ13
64 lysogeny leads to disruption of *hlb* and loss of β-hemolytic activity, with excision
65 reconstituting an intact *hlb* gene (5, 7, 8).

66 Phage Φ13 also carries the *iec* immune evasion cluster including several genes
67 involved in escape from the host innate immune response: *scn*, *chp* and *sak* (9, 10).
68 Natural mobility has been shown in vivo for Φ13-related phages during murine skin
69 colonization and rabbit invasive infection as well as in isolates from cystic fibrosis
70 patients and healthy individuals (5, 11-13). Additionally, among *S. aureus* isolates from
71 recurrent furunculosis, 45% produced β-hemolysin compared to only 19% of those
72 from nasal colonization (14).

73 Given the importance of phage Φ13 excision on β-hemolytic activity, we wished
74 to study the effect of the presence or absence of phage Φ13 on *S. aureus* virulence
75 during systemic infection in three different configurations that had not been
76 previously studied:

77 -a) preventing phage excision and consequently β-hemolytic activity

78 -b) absence of phage Φ13 leading to continuous β-hemolytic activity

79 -c) simultaneous presence of phage Φ13 and a functional *hlb* gene.

80 We show that timely excision of the Φ13 prophage is essential for pathogenesis,
81 with early β-hemolysin production leading to a significant increase in virulence and
82 elevated levels of the pro-inflammatory cytokine IL-6. Conversely, preventing phage
83 Φ13 excision significantly lowers staphylococcal virulence.

84 **RESULTS**

85

86 **Mobility dynamics of *Staphylococcus aureus* prophages**

87

88 *S. aureus* strain HG001, a derivative of sepsis isolate NCTC 8325 (15), carries prophages
89 Φ11, Φ12 and Φ13 (7, 16). Specific oligonucleotide primer pairs were designed to detect
90 the presence or absence of each prophage (Supplementary Table 2). Using
91 chromosomal DNA from a closely related strain cured of all phages, SH1000, an
92 amplicon corresponding to the native bacterial locus without Φ13 (oligonucleotide
93 pair OMA7/OMA9, hybridizing on either side of the *attB* site, Supplementary Fig. 1A)
94 was detected, but no amplification occurred with oligonucleotides specific for Φ13
95 insertion (OMA7/OMA8; Supplementary Fig. 1B). With the HG001 Φ13 lysogen strain,
96 both types of amplicon were generated by PCR, suggesting spontaneous Φ13 excision
97 within the bacterial population (Supplementary Fig. 1B). We quantified relative
98 prophage levels within the bacterial population by qRT-PCR during growth under
99 optimal laboratory conditions (TSB at 37°C with aeration). Our results indicate that
100 prophage Φ11 is highly mobile with approximately 10% of cells lacking the phage
101 whereas Φ12 was much more stable with less than 0.01% of non-lysogen cells (Fig. 1A).
102 Interestingly, the Φ13 prophage was lost in about 0.5% of the population under these
103 growth conditions (Fig. 1A).

104

105 **Excision of prophage Φ13 is increased *in vivo***

106

107 As shown above, prophage Φ13 is spontaneously excised during growth under
108 laboratory conditions. Since this phage carries genes encoding the SAK staphylokinase
109 virulence factor, as well as SCIN and CHIP, involved in escape from the innate
110 immune response (17), we examined Φ13 excision frequency during the infectious
111 process.

112 We generated a strain carrying the *aad*(9) spectinomycin resistance gene inserted
113 within the Φ13 genome of the HG001 strain (see Materials and Methods, and
114 Supplementary Table 1 strain ST1387). We verified that the *aad*(9) cassette did not
115 interfere with Φ13 stability during growth in vitro. In the ST1387 strain (HG001Φ13 -
116 *aad*(9)), the prophage excision frequency was 0.58% ± 0.05%, which is comparable to

117 the excision rate observed in the wild-type HG001 strain (0.59% ± 0.05%), as
118 determined by qRT-PCR. Four days following sub-lethal (2 x 10^7 c.f.u.) intravenous
119 inoculation with *S. aureus* strain ST1387, mice were sacrificed and kidneys collected
120 for c.f.u. counts. Out of 25 harvested kidneys, 18 were colonized by a mixed bacterial
121 population with respect to Φ13 lysogeny (Fig.1B). In some mice a single kidney was
122 colonized with a mixed population with the other only by Φ13 lysogens, suggesting
123 that loss of Φ13 is a *post facto* event to kidney colonization. The average loss of Φ13 was
124 around 50% in the 18 kidneys colonized with a mixed bacterial population (Fig. 1C), a
125 significant increase over the spontaneous excision rate of 0.5% observed during
126 growth *in vitro*. The specific in vivo dynamics of prophage content suggests either an
127 induction of Φ13 excision in response to conditions encountered during infection or a
128 selective advantage for the non-lysogenic strain, potentially due to enhanced fitness
129 during kidney colonization through loss of the prophage.
130
131 **Excision of prophage Φ13 is essential for the *S. aureus* infectious process**
132
133 Increased prophage Φ13 excision during infection suggests it may impact virulence.
134 The Φ13 SAOUHSC-*02293* gene, referred to henceforth as *int*, encodes a protein highly
135 similar to tyrosine recombinase integrases such as Int of phage lambda (16, 18). We
136 deleted the entire coding sequence of the Φ13 *int* gene in *S. aureus* strain HG001 in
137 order to prevent excision, locking the prophage within the bacterial chromosome. We
138 also constructed a strain where the entire Φ13 genome is deleted, restoring an intact
139 and functional *hlb* gene (see Materials and Methods). These mutations had no effect on
140 bacterial growth *in vitro* (Supplementary Fig. 2). β-hemolytic activity following Φ13
141 excision was detected on sheep blood agar plates as a distal cold-inducible halo of
142 partial hemolysis (indicated by the white arrow in Fig. 2A).
143 As shown in Fig. 2B, the frequency of Φ13 excision in the Δ*int* mutant is lowered
144 more than 1000-fold as compared to that of the wild type strain (0.6%), confirming the
145 essential role of Int in Φ13 excision. Full complementation of the Δ*int* mutant was
146 obtained by expressing the *int* gene from the Pprot constitutive promoter in the
147 pMK4Pprot-*int* plasmid (Fig. 2B).
148 We next examined the effect on *S. aureus* virulence of either the absence of
149 prophage Φ13 (HG001ΔΦ13 strain, intact *hlb* gene) or the lack of Φ13 excision

150 (HG001Δ*int* strain, *hlb* gene disrupted). As shown in Fig. 3A, using a systemic model
151 of murine infection (5 X 10^7 c.f.u. intravenous injection), the absence of Φ13 with a
152 resulting intact *hlb* gene led to acute virulence with the rapid death of infected animals
153 (50% mortality 24 h post-infection for the ΔΦ13 strain vs. six days for the wild type
154 strain), and more than 90% mortality at the end of the assay (ten days post-infection).
155 Conversely, when Φ13 excision is abolished (Δ*int* strain), *S. aureus* virulence is strongly
156 reduced compared to the wild type strain (31% mortality at the end of the assay, *vs*
157 63%). These results indicate that Φ13 excision and its timing are crucial parameters for
158 the *S. aureus* infectious process.
159
160 **Φ13 dynamics are involved in organ damage during infection**
161
162 To understand the effect of Φ13 dynamics on *S. aureus* virulence, we measured
163 bacterial colonization, and evaluated the kidney lesions of infected mice by
164 histopathological analysis. Mice were inoculated intravenously with sub-lethal
165 concentrations of *S. aureus* cells (approximately 2 X 10^7 c.f.u.). At six days post-infection,
166 mice were sacrificed and one kidney was fixed for histopathological analysis and the
167 other homogenized for c.f.u. counts. Kidney bacterial loads for the parental HG001
168 strain and the HG001ΔΦ13 and HG001Δ*int* mutants were not significantly different
169 (approximately 5 X 10^7 c.f.u. per kidney; Supplementary Fig. 3). However,
170 histopathological analysis revealed nephritis (very probably embolic nephritis) with
171 significantly varying degrees of severity between mice infected with the parental
172 HG001 strain or the ΔΦ13 and Δ*int* mutants. At six days post-infection, mice inoculated
173 with the wild type strain generally displayed mild to moderate nephritis (5/6 mice) or
174 multifocal inflammatory infiltrates (macrophages and other mononucleated cells) in
175 the renal cortex (1/6 mouse) (Fig. 3B1 and 3B2). In contrast, the ΔΦ13 strain leads to
176 more severe nephritis (5/6 mice), with neutrophilic inflammation forming multifocal
177 abscesses, extension to tubules and interstitium, and ischemic necrosis of the papillae
178 (Fig. 3B3 and 3B4). Mice infected with the Δ*int* strain displayed less severe lesions, with
179 mononuclear cell infiltrates mostly in the cortex (4/6 mice) or mild to moderate (1/6
180 mouse) or marked (1/6 mouse) nephritis (Fig. 3B5 and 3B6).

181 These results show that Φ13 dynamics and correlated β-hemolysin production
182 are not essential for host colonization but instead are key factors in host organ damage
183 during infection.
184
185 **Φ13 excision triggers host inflammatory response in infected THP-1 cells**
186
187 Given the major impact of Φ13 excision on virulence and inflammation, we tested its
188 effect on induction of the cellular inflammatory response using human monocytic
189 THP-1 cells. We compared the bacterial internalization capacity of THP-1 cells, the
190 intracellular viability of bacterial cells and the induction of inflammatory markers
191 following infection with the parental HG001 strain and the ΔΦ13 and Δ*int* mutants.
192 THP-1 differentiated macrophages were very efficient for *S. aureus* phagocytosis
193 regardless of prophage content, with nearly 100% of bacteria internalized with a m.o.i.
194 (multiplicity of infection) of 10 after 2 hours (Supplementary Fig. 4A). Intracellular
195 survival was not significantly different for the three strains with approximately 10%
196 survival after 24 h post infection and less than 5% after 48 h (Supplementary Fig. 4B).
197 To measure induction of the inflammatory response, duplicate aliquots of infected
198 THP-1 cells were frozen 24 h post-infection, treated to recover cellular RNA and
199 induction of inflammatory cytokine genes measured by qRT-PCR. We measured
200 induction of three pro-inflammatory cytokines previously shown to be induced by
201 *S. aureus* infection, TNFα, IL-1β and IL-6 (19). Although there was no significant
202 difference in induction levels of TNFα and Pro-IL-1β for the three strains, IL-6 gene
203 expression was strongly increased when THP-1 cells were infected with the ΔΦ13
204 strain as compared to the HG001 strain and the Δ*int* mutant (Fig. 4). Thus, lysogeny
205 by Φ13 and the concomitant loss of β-hemolytic activity appear to down-regulate the
206 inflammatory response through lower induction of the pro-inflammatory cytokine IL-
207 6.
208
209 **Impact of *hlb* on *S. aureus* virulence**
210
211 Taken together the results shown above suggest a major role of β-hemolysin
212 production in the increased virulence of the ΔΦ13 strain. To test this hypothesis, we
213 compared the virulence of the ΔΦ13 strain, which produces β-hemolysin, with the

214 virulence of the ΔΦ13Δ*hlb* strain in which the *hlb* gene has also been deleted. As shown
215 in Fig. 5A, 44% of mice infected by the ΔΦ13Δ*hlb* strain survived at nine days post-
216 infection, whereas survival of mice infected by the strain producing β-hemolysin
217 (ΔΦ13) was only 14%, indicating that it is the major factor responsible for the effect of
218 Φ13 excision on *S. aureus* virulence. To test the contribution of Φ13 in virulence, we
219 constructed a strain where both Φ13 and an intact *hlb* gene are present (Δ*int hlb*
220 complemented strain; see Materials and Methods, and Supplementary Table 1). As
221 shown in Fig. 5B, mouse mortality caused by the ΔΦ13 strain producing β-hemolysin
222 but lacking the Φ13 prophage was essentially the same as that following infection by
223 the Δ*int hlb* complemented strain (with both the Φ13 prophage and a functional *hlb*
224 gene). This result confirms the major role of Φ13 dynamics in *S. aureus* virulence by
225 controlling timing of β-hemolysin production during the infectious process.
226

227 **DISCUSSION**

228 *Staphylococcus aureus* is a highly successful human pathogen with a sophisticated
229 arsenal of virulence factors whose production is tightly controlled by multiple
230 regulatory networks, such as two-component systems (20). Further fine-tuning is
231 provided by mobile genetic elements such as pathogenicity islands (SaPI), plasmids,
232 transposons, staphylococcal cassette chromosomes (SCC) and bacteriophages
233 conferring additional virulence factors or antibiotic resistance genes (21). Prophages
234 are widely distributed amongst *S. aureus* strains. Among these, the Φ13 *S. aureus*
235 prophage is inserted within the *hlb* gene encoding β-hemolysin and carries at least
236 three genes involved in host interactions and escape from the immune response,
237 known as the immune evasion cluster (IEC): *sak*, encoding staphylokinase, involved in
238 converting host plasminogen to active plasmin, *scn*, encoding a staphylococcal
239 complement inhibitor, and *chp*, encoding a neutrophil and monocyte chemotaxis
240 inhibitory protein (9). The Φ13 *hlb*-converting prophage family is present in
241 approximately 90% of *S. aureus* clinical isolates (9).

242 β-hemolysin is a sphingomyelinase that can lyse proliferating human
243 lymphocytes, contributing to the host immune evasion (22). Independently of its pore
244 forming activity, β -hemolysin has a biofilm ligase effect by forming a nucleoprotein
245 matrix both in vitro and during infectious endocarditis (23, 24). It has also been shown
246 that Hlb favors mouse skin colonization (12). We noted that *S. aureus* cells isolated
247 from infected mice frequently displayed β-hemolytic activity due to *in vivo* excision of
248 the Φ13 prophage. This prompted us to examine the effect of phage mobility on host
249 pathogen interactions. Our results indicate that mobility of this prophage is required
250 for full virulence of *S. aureus* as part of the time-course of the infectious process. We
251 identified and inactivated the potential integrase gene of this prophage, effectively
252 locking the prophage within the *S. aureus* genome by preventing its excision, and
253 showed that this leads to strongly decreased virulence, with 70% of the mice still
254 surviving after 10 days. Conversely, a strain lacking the Φ13 prophage exhibited
255 greater virulence than the wild type strain, with 50% of infected mice succumbing
256 within the first day of infection, compared to six days for the wild-type strain. These
257 Φ13-associated virulence traits are not correlated to differences in the strain's ability to
258 colonize the host, as bacterial loads in the infected kidneys were similar regardless of
259 the strain's lysogenic status. However, kidney damage following infection was

strongly associated with the presence of Φ13, showing a clear gradient where a lower proportion of lysogenic bacteria resulted in more severe tissue lesions. In a human monocyte (THP-1) infection model used to assess inflammatory response, we found that the non-lysogenic strain significantly increased the production of the pro-inflammatory cytokine IL-6. IL-6 triggers the release of acute-phase response proteins into the bloodstream, leading to a systemic inflammatory response (25). It is also considered a key biomarker for predicting poor outcomes in sepsis patients and is a promising target for inhibitors to help mitigate the adverse effects of inflammation (19, 26). The induction of IL-6 by the non-lysogenic strain may be linked to its heightened virulence and the significant neutrophil recruitment observed at the inflammation site, as shown by the histopathological analysis of infected kidneys.

The exact trigger causing excision of Φ13 during infection remains to be established. Interestingly, our observations show that after intravenous infection, kidneys of the same mouse can be colonized differently, one kidney by a lysogenic population, while the other harbors a mixed population. This suggests that Φ13 excision is likely induced in the kidneys following colonization rather than during the initial spread of bacteria through the bloodstream. Interestingly, a previous study using a rabbit infection model found that bacteria producing β-hemolysin emerged during organ colonization, but this was not observed in the bacterial population recovered from the bloodstream (11). Stress conditions activating the SOS response are known to induce prophage excision. However, despite many attempts, we were not able to induce Φ13 excision from the bacterial chromosome through treatment with Mitomycin C as SOS-inducing agent. Similar results were previously described with a Newman strain carrying the closely related *hlb*-converting prophage, ΦNM3 (27). More recently, it has been demonstrated that exposure to oxidative stress (such as hydrogen peroxide) and biofilm growth conditions promote the excision of ΦSA3mw (28). This may correlate with our in vivo observations, i.e., that phage induction occurs after organ colonization, under biofilm development conditions.

Epidemiological studies have shown that *hlb*-converting prophages are more commonly found in strains colonizing humans (from nasal swabs) than in invasive strains (isolated from blood) (3). Additionally, Φ13-derivative carriers are significantly more frequent in human *S. aureus* isolates than in animal strains (29). These *hlb*-converting phages not only inactivate *hlb* but also carry virulence genes, including an immune evasion cluster (IEC) (9). The Sak, SCIN, and CHIPS determinants encoded

294 by this cluster play crucial roles in modulating neutrophil chemotaxis, bacterial
295 phagocytosis, and killing (17). However, their activity is highly specific, primarily
296 targeting the human immune system (30-32). This specificity of the Φ13-derivative IEC
297 in counteracting the human immune response likely contributes to the greater
298 prevalence of *hlb*-converting prophages in human *S. aureus* strains.

299 Interestingly, we demonstrated using a murine systemic infection model, that the
300 *hlb* gene is the major determinant responsible for the increased virulence observed in
301 the absence of the Φ13 phage. When Hlb is produced, no effect of Φ13 alone was
302 observed (Fig. 5B), likely because the strain is already highly virulent due to constant
303 Hlb production. However, in the absence of *hlb*, the presence of Φ13 led to lowered
304 mouse mortality (Fig. 3A and 5A). While the immune evasion factors encoded by Φ13
305 have been described as human-specific, it cannot be excluded that they may also
306 exhibit some activity during mouse colonization. Alternatively, Φ13 may encode
307 uncharacterized proteins that could modulate *S. aureus* virulence.

308 Excision of Φ13 and the chromosomal rearrangement reconstituting an intact *hlb*
309 gene can be viewed as a timing device, ensuring that the bacteria first colonize the host,
310 benefiting from the immune evasion cluster proteins encoded by the prophage, with
311 production of β-hemolysin and host tissue damage occurring once the bacteria have
312 reached a threshold level, in agreement with the temporal control of *Staphylococcus*
313 *aureus* virulence factors (33). One of the first examples of prophage excision as a timing
314 device for a developmental process is the *skin* element whose excision leads to a
315 chromosomal rearrangement reconstituting the gene encoding the Sigma K sigma
316 factor, essential for *Bacillus subtilis* sporulation (34, 35).

317 As demonstrated in this study and supported by the literature, the
318 heterogeneity within *S. aureus* populations with respect to *hlb*-converting prophages
319 appears to be a common trait. This could be seen as a bet-hedging strategy, allowing
320 the bacteria to retain the ability to produce both immune evasion proteins (in the
321 lysogenic population) and the potent Hlb cytotoxin (in the non-lysogenic cells).
322 Additionally, since both β-hemolysin and the immune evasion cluster proteins
323 encoded by the prophage are secreted, it is plausible that functional complementation
324 may occur within a mixed population of lysogenic and non-lysogenic bacteria. Similar
325 dual strategies have been observed before, where bistability leads to cell-to-cell
326 variation in gene expression (36, 37). This mixed population with distinct genetic

327 content would be well-equipped to resist host defenses during colonization as well as
328 causing cellular damage.

329

330 **MATERIALS AND METHODS**

331 **Bacterial strains and growth media**

332

333 *Escherichia coli* K12 strain DH5α™ (Invitrogen) was used for cloning experiments.
334 *Staphylococcus aureus* strain HG001, derived from strain NCTC 8325 by repairing the
335 mutated *rsbU* gene (15), was used for genetic and functional studies. Plasmids were
336 first transformed into the restriction deficient *S. aureus* strain RN4220 before
337 introduction into the HG001 or derivative strains. *E. coli* strains were grown in LB
338 medium with ampicillin (100 μg/mL) added when required. *S. aureus* strains and
339 plasmids used in this study are listed in Supplementary Table 1. *S. aureus* strains were
340 grown in Trypticase Soy Broth (TSB; Difco) supplemented with chloramphenicol (10
341 μg/mL) or erythromycin (1 μg/mL) when required. *E. coli* and *S. aureus* strains were
342 transformed by electroporation using standard protocols (38) and transformants were
343 selected on LB or Trypticase Soy Agar (TSA; Difco) plates, respectively, with the
344 appropriate antibiotics.

345

346 **DNA manipulations**

347

348 Oligonucleotides used in this study were synthesized by Eurofins Genomics and are
349 listed in Supplementary Table 2. *S. aureus* chromosomal DNA was isolated using the
350 MasterPure™ Gram-positive DNA purification Kit (Epicentre Biotechnologies).
351 Plasmid DNA was isolated using a QIAprep Spin Miniprep kit (Qiagen) and PCR
352 fragments were purified using the Qiaquick PCR purification kit (Qiagen). T4 DNA
353 ligase and restriction enzymes, PCR reagents and Q5 high-fidelity DNA polymerase
354 (New England Biolabs) were used according to the manufacturer's recommendations.
355 Nucleotide sequencing of plasmid constructs was carried out by Eurofins Genomics .

356

357 **Plasmids and mutant strain construction**

358

359 Construction of the ΔΦ13 mutant strain was carried out by cloning an 1800 bp DNA
360 fragment centered around the *attB* site, generated by PCR using oligonucleotides
361 OSA418 and OSA419 and chromosomal DNA from the SH1000 strain (a NCTC8325-4
362 derivative cured for prophages), between the *Bam*HI and *Eco*RI sites of the pMAD
363 vector (39), to give plasmid pMAD-Φ13. For deletion of the Φ13 integrase (*int*; *saouhsc-*

364 *02239*), DNA fragments corresponding to the *int* upstream and downstream regions
365 were generated using oligonucleotides OSA411/OSA412 (900 bp) and
366 OSA413/OSA414 (820 bp) cloned between the pMAD *Bam*HI and *Nco*I sites. The *aad*(9)
367 spectinomycin resistance gene (40) was inserted in the center of the 23 nt intergenic
368 region between the convergent Φ13 *saouhsc-02232* and *saouhsc-02233* genes, to avoid
369 any polar effects on transcription. DNA fragments corresponding to the regions
370 upstream and downstream from the insertion site were generated by PCR using
371 primers OSA508/OSA509 and OSA510/OSA511, respectively, and primers
372 OSA299/OSA470 for the *aad*(9) cassette with plasmid pIC333 (41) as the DNA matrix.
373 The DNA fragments were cloned into pMAD using the *Bam*HI/*Sal*I sites for the
374 upstream fragment, *Sal*I/*Nco*I for the *aad*(9) cassette, and the *Nco*I/*Bgl*II sites for the
375 downstream fragment, generating plasmid pMAD-Φ13*aad*(9). For deletion of *hlb*, we
376 generated upstream and downstream fragments by PCR using oligonucleotides
377 OSA442/OSA443 (884 bp) and OSA444/OSA445 (889 bp) respectively. These
378 fragments were introduced into pMAD between the *Bam*HI and *Eco*RI sites, thus
379 generating the pMAD-*hlb* plasmid. To introduce a functional *hlb* allele into the Φ13
380 lysogenic strain, a pMAD-*hlb*comp plasmid was constructed to place the intact *hlb* gene
381 upstream from the Φ13 genome. A PCR fragment including the *hlb* upstream region
382 and the *hlb* intact gene (1760 bp) was generated using the OSA418 and OSA573 primers
383 and the SH1000 genomic DNA as matrix and cloned into pMAD using the *BamH*I and
384 *Sal*I restriction sites. A second PCR fragment corresponding to the part of Φ13 adjacent
385 to *att*L was generated with the OSA574-575 primers and cloned between the *Sal*I and
386 *Bgl*II restriction sites of pMAD.
387 Plasmids were introduced by electroporation into *S. aureus* strain RN4220, and
388 transformants selected at 30°C on TSA plates containing erythromycin and 5-bromo-
389 4-chloro-3-indolyl-β-D-galactopyranoside (X-Gal) (100 μg/mL). Plasmids were then
390 introduced into strain HG001 and integration and excision performed as previously
391 described (39), yielding strains HG001ΔΦ13, HG001Δ*int*, and HG001Φ13-aad(9) and
392 into strain HG001ΔΦ13 for pMAD-*hlb* and HG001Δ*int* for pMAD-*hlb*comp to give
393 strains HG001Δ*int hlb*comp and HG001ΔΦ13Δ*hlb*.
394 Plasmid pMK4Pprot-*int* was used for complementation of the Δ*int* mutant and
395 constructed by cloning the entire *int* coding sequence (amplicon OSA446/OSA447)
396 under the control of the constitutive P*prot* promoter (42).
397

398 **Prophage content measurement by quantitative real time PCRs (qRT-PCRs)**

399

400 Strains were grown overnight in TSB at 37°C, with aeration. Cells were pelleted by
401 centrifugation (2 min, 20,800 *g*) from 2 mL culture samples and genomic DNA
402 extracted using the MasterPure™ Gram Positive DNA Purification Kit (Tebu-Bio).
403 Oligonucleotides were designed with the BEACON Designer 4.02 software (Premier
404 Biosoft International, Palo Alto, CA) to synthesize 100-200 bp amplicons (see
405 Supplementary Table 2). Quantitative real-time PCRs (qRT-PCRs) and critical
406 threshold cycles (CT) were performed and determined using the SsoFast™ EvaGreen
407 Supermix (Bio-Rad, Hercules, CA). All assays were performed using quadruplicate
408 technical replicates, and repeated with three independent biological samples, with one
409 representative experiment shown. Prophage loss frequency was calculated using the
410 formula: $1/(1+2^{\Delta Ct})$, $\Delta Ct = Ct_{phage\ negative} - Ct_{phage\ positive}$ derived from the ΔCt method (43).

411

412 **Hemolysis detection**

413

414 Bacteria were grown overnight in TSB at 37°C with aeration. Culture aliquots (3 µl)
415 were spotted on Columbia plates containing 5% sheep blood (COS, Biomerieux
416 Craponne). Plates were incubated for 24h at 37°C and transferred to 4°C for an
417 additional 24h to for detection of β-hemolysis (44).

418

419 **THP-1 infection experiments**

420

421 THP-1 monocytes were maintained as previously described (45). Differentiation and
422 adherence were obtained by incubation with Phorbol 12-Myristate 13-Acetate (PMA,
423 50 ng/mL) during 4 days at 37°C in a 5%CO_2 atmosphere. Bacterial uptake
424 experiments and survival assays were carried out as previously described (46). Briefly,
425 bacteria were grown in TSB until OD_{600nm} = 1. Cultures were washed in PBS and
426 adjusted to the desired inoculum in RPMI 1640 medium (Gibco), and c.f.u. counts
427 determined by plating serial dilutions on TSA plates. Differentiated THP-1
428 macrophages were incubated with bacteria (m.o.i. = 10) in RPMI 1640 at 37°C with 5%
429 CO2 for 1 h to allow bacterial phagocytosis. They were then washed with RPMI and
430 incubated in RPMI-10% Fetal Calf Serum with streptomycin (100 µg/mL), penicillin
431 (100 U/mL), and gentamycin 40 µg/mL to eliminate extracellular bacteria. At the

432 indicated times, infected macrophages were washed once with RPMI and lysed by
433 incubation in ice-cold water for 15 min and c.f.u. counts were determined by plating
434 serial dilutions on TSA plates. For cytokine gene expression studies by qRT-PCR, THP-
435 1 cells were frozen at -20°C 24h post-infection. Total RNA was extracted using a
436 RNeasy mini kit (Qiagen, CA, USA). Cytokine gene expression was analysed by qRT-
437 PCR using the StepOnePlus real-time PCR system (Applied Biosystems). Primers used
438 for qRT-PCR were TNFα, IL6, pro-IL1beta and HPRT as the reference gene. The qRT-
439 PCRs were performed by Taqman and results presented as relative quantification of
440 gene expression using the $2^{-\Delta\Delta CT}$ method.
441
442 **Animal experiments**
443
444 Seven-week-old female *RjOrl:SWISS* mice (Janvier Labs) were inoculated
445 intravenously with the specified *S. aureus* strains. To analyze Φ13 excision during the
446 infectious process, mice were infected with a sublethal dose (2×10^7 c.f.u.) of the Φ13-
447 *aad*(9) strain. Mice were sacrificed four days post-infection and kidneys harvested and
448 homogenized for c.f.u. determination following dilution and plating on TSA and TSA
449 with spectinomycin (100 µg/mL). The rate of prophage excision was calculated as
450 [(c.f.u. on TSA) - (c.f.u. on TSA+spectinomycin)]/(c.f.u. on TSA).
451 Strain HG001 and the Δ*int*, ΔΦ*13*, ΔΦ*13*Δ*hlb* and Δ*int hlb*comp mutants were used
452 for survival studies. Groups of seven mice were injected in the caudal lateral vein with
453 5×10^7 c.f.u. per mouse in 0.2 mL. Survival was monitored daily for 9 days following
454 infection and three independent experiments were carried out. To measure kidney
455 colonization and histopathological analysis, mice were infected intravenously with a
456 sublethal dose (1×10^7 c.f.u.) of the HG001 parental and Δ*int* and ΔΦ*13* mutant strains
457 (six mice for each strain). At six days post-infection, kidneys were collected and for
458 each mouse, bacterial c.f.u. counts were carried out using one kidney and
459 histopathological observations were done on the other kidney. For histopathology,
460 kidneys were removed and immediately fixed in 10% neutral buffered formalin. After
461 48 h of fixation, the kidneys were longitudinally sectioned through the hilus in order
462 to obtain the renal cortex, medulla, crest, and pelvis on the same section. These
463 samples were embedded in paraffin, and 4-µm sections were cut and stained with
464 hematoxylin and eosin (lesion description) and Gram (bacterial detection).
465

466 **Ethics statement**

467

468 Animal experiments were carried out at the Institut Pasteur according to European
469 Union guidelines for handling of laboratory animals
470 (http://ec.europa.eu/environment/chemicals/lab_animals/index_en.htm).
471 Animals were monitored daily with a particular attention for any signs of distress.
472 Protocols used were approved by the Institut Pasteur ethics committee (dap160057).

473

474 **Statistical analysis**

475

476 Statistical significance in survival experiments was determined using the log-rank,
477 Mantel–Cox test, and significance across means was carried out using *t*-test (Graph-
478 Pad Prism Software).

479

ACKNOWLEDGMENTS

We are grateful to Grégory Jouvion for the histopathological analysis, Patrick Trieu-Cuot, in whose lab this work was carried out, and Shaynoor Dramsi for helpful discussion. All authors have read and agreed to the submitted version of the manuscript.

FUNDING

This work was supported by funds from Institut Pasteur, CNRS, and Vaincre La Mucoviscidose Association (Grant «Phage induction, a novel essential factor for *Staphylococcus aureus* infections?»).

AUTHOR CONTRIBUTIONS

Conceptualization: Sarah Dubrac, Lhousseine Touqui, Tarek Msadek.
Data curation: Olivier Poupel, Sarah Dubrac, Lhousseine Touqui, Tarek Msadek.
Formal analysis: Sarah Dubrac, Lhousseine Touqui, Tarek Msadek.
Funding acquisition: Sarah Dubrac, Lhousseine Touqui, Tarek Msadek.
Investigation: Olivier Poupel, Gérard Kénanian, Charlotte Abrial, Sarah Dubrac.
Methodology: Olivier Poupel, Sarah Dubrac.
Project administration: Tarek Msadek, Sarah Dubrac.
Resources: Tarek Msadek, Sarah Dubrac.
Supervision: Tarek Msadek, Sarah Dubrac.
Validation: Tarek Msadek, Sarah Dubrac.
Writing – original draft: Tarek Msadek, Sarah Dubrac.
Writing – review & editing: Tarek Msadek, Sarah Dubrac.

ADDITIONAL FILES

The following material is available online.

Supplemental Material

Supplemental Figures and Tables. Fig. S1–S4 and Tables S1–S2.

517 **REFERENCES**

518

519 1. Piewngam P, Otto M. 2024. *Staphylococcus aureus* colonisation and strategies for
520 decolonisation. Lancet Microbe 5:e606-e618.
521 2. Fitzgerald JR, Sturdevant DE, Mackie SM, Gill SR, Musser JM. 2001.
522 Evolutionary genomics of *Staphylococcus aureus*: insights into the origin of
523 methicillin-resistant strains and the toxic shock syndrome epidemic. Proc Natl
524 Acad Sci USA 98:8821-6.
525 3. Goerke C, Pantucek R, Holtfreter S, Schulte B, Zink M, Grumann D, Broker BM,
526 Doskar J, Wolz C. 2009. Diversity of prophages in dominant *Staphylococcus*
527 *aureus* clonal lineages. J Bacteriol 191:3462-8.
528 4. Xia G, Wolz C. 2014. Phages of *Staphylococcus aureus* and their impact on host
529 evolution. Infect Genet Evol 21:593-601.
530 5. Goerke C, Wirtz C, Fluckiger U, Wolz C. 2006. Extensive phage dynamics in
531 *Staphylococcus aureus* contributes to adaptation to the human host during
532 infection. Mol Microbiol 61:1673-85.
533 6. Feiner R, Argov T, Rabinovich L, Sigal N, Borovok I, Herskovits AA. 2015. A
534 new perspective on lysogeny: prophages as active regulatory switches of
535 bacteria. Nat Rev Microbiol 13:641-50.
536 7. Iandolo JJ, Worrell V, Groicher KH, Qian Y, Tian R, Kenton S, Dorman A, Ji H,
537 Lin S, Loh P, Qi S, Zhu H, Roe BA. 2002. Comparative analysis of the genomes
538 of the temperate bacteriophages phi 11, phi 12 and phi 13 of *Staphylococcus*
539 *aureus* 8325. Gene 289:109-18.
540 8. Coleman DC, Sullivan DJ, Russell RJ, Arbuthnott JP, Carey BF, Pomeroy HM.
541 1989. *Staphylococcus aureus* bacteriophages mediating the simultaneous
542 lysogenic conversion of beta-lysin, staphylokinase and enterotoxin A:
543 molecular mechanism of triple conversion. J Gen Microbiol 135:1679-97.
544 9. van Wamel WJ, Rooijakkers SH, Ruyken M, van Kessel KP, van Strijp JA. 2006.
545 The innate immune modulators staphylococcal complement inhibitor and
546 chemotaxis inhibitory protein of *Staphylococcus aureus* are located on beta-
547 hemolysin-converting bacteriophages. J Bacteriol 188:1310-5.
548 10. Rohmer C, Wolz C. 2021. The role of hlb-converting bacteriophages in
549 *Staphylococcus aureus* host adaption. Microb Physiol 31:109-122.
550 11. Salgado-Pabon W, Herrera A, Vu BG, Stach CS, Merriman JA, Spaulding AR,
551 Schlievert PM. 2014. *Staphylococcus aureus* beta-toxin production is common in

552 strains with the beta-toxin gene inactivated by bacteriophage. J Infect Dis
553 146:784-92.
554 12. Katayama Y, Baba T, Sekine M, Fukuda M, Hiramatsu K. 2013. Beta-hemolysin
555 promotes skin colonization by *Staphylococcus aureus*. J Bacteriol 195:1194-203.
556 13. Goerke C, Matias y Papenberg S, Dasbach S, Dietz K, Ziebach R, Kahl BC, Wolz
557 C. 2004. Increased frequency of genomic alterations in *Staphylococcus aureus*
558 during chronic infection is in part due to phage mobilization. J Infect Dis
559 189:724-34.
560 14. Hedstrom SA, Malmqvist T. 1982. Sphingomyelinase activity of *Staphylococcus*
561 *aureus* strains from recurrent furunculosis and other infections. Acta Pathol
562 Microbiol Immunol Scand B 90:217-20.
563 15. Herbert S, Ziebandt AK, Ohlsen K, Schafer T, Hecker M, Albrecht D, Novick R,
564 Gotz F. 2010. Repair of global regulators in *Staphylococcus aureus* 8325 and
565 comparative analysis with other clinical isolates. Infect Immun 78:2877-89.
566 16. Gillaspy AF, Worrell V, Orvis J, Roe BA, Dyer DW, Iandolo JJ. 2006. The
567 *Staphylococcus aureus* NCTC 8325 Genome, p 381-412. *In* Fischetti VA, Novick
568 RP, Ferretti JJ, Portnoy DA, Rood JI (ed), Gram-Positive Pathogens, 2nd ed.
569 ASM Press, Washington, DC.
570 17. Rooijakkers SH, van Kessel KP, van Strijp JA. 2005. Staphylococcal innate
571 immune evasion. Trends Microbiol 13:596-601.
572 18. Nunes-Duby SE, Kwon HJ, Tirumalai RS, Ellenberger T, Landy A. 1998.
573 Similarities and differences among 105 members of the Int family of site-specific
574 recombinases. Nucleic Acids Res 26:391-406.
575 19. van den Berg S, Laman JD, Boon L, ten Kate MT, de Knegt GJ, Verdijk RM,
576 Verbrugh HA, Nouwen JL, Bakker-Woudenberg IA. 2013. Distinctive cytokines
577 as biomarkers predicting fatal outcome of severe *Staphylococcus aureus*
578 bacteremia in mice. PLoS One 8:e59107.
579 20. Haag AF, Bagnoli F. 2017. The role of two-component signal transduction
580 systems in *Staphylococcus aureus* virulence regulation. Curr Top Microbiol
581 Immunol 409:145-198.
582 21. Lindsay JA. 2010. Genomic variation and evolution of *Staphylococcus aureus*. Int
583 J Med Microbiol 300:98-103.
584 22. Huseby M, Shi K, Brown CK, Digre J, Mengistu F, Seo KS, Bohach GA,
585 Schlievert PM, Ohlendorf DH, Earhart CA. 2007. Structure and biological
586 activities of beta toxin from *Staphylococcus aureus*. J Bacteriol 189:8719-26.

587 23. Herrera A, Vu BG, Stach CS, Merriman JA, Horswill AR, Salgado-Pabon W,
588 Schlievert PM. 2016. *Staphylococcus aureus* beta-toxin mutants are defective in
589 biofilm ligase and sphingomyelinase activity, and causation of infective
590 endocarditis and sepsis. Biochemistry 55:2510-7.
591 24. Huseby MJ, Kruse AC, Digre J, Kohler PL, Vocke JA, Mann EE, Bayles KW,
592 Bohach GA, Schlievert PM, Ohlendorf DH, Earhart CA. 2010. Beta toxin
593 catalyzes formation of nucleoprotein matrix in staphylococcal biofilms. Proc
594 Natl Acad Sci USA 107:14407-12.
595 25. Tanaka T, Narazaki M, Kishimoto T. 2014. IL-6 in inflammation, immunity, and
596 disease. Cold Spring Harb Perspect Biol 6:a016295.
597 26. Cao YZ, Tu YY, Chen X, Wang BL, Zhong YX, Liu MH. 2012. Protective effect
598 of Ulinastatin against murine models of sepsis: inhibition of TNF-alpha and IL-
599 6 and augmentation of IL-10 and IL-13. Exp Toxicol Pathol 64:543-7.
600 27. Bae T, Baba T, Hiramatsu K, Schneewind O. 2006. Prophages of *Staphylococcus*
601 *aureus* Newman and their contribution to virulence. Mol Microbiol 62:1035-47.
602 28. Tran PM, Feiss M, Kinney KJ, Salgado-Pabon W. 2019. ØSa3mw prophage as a
603 molecular regulatory switch of *Staphylococcus aureus* β-toxin production. J
604 Bacteriol 201:e00766-18.
605 29. Verkaik NJ, Benard M, Boelens HA, de Vogel CP, Nouwen JL, Verbrugh HA,
606 Melles DC, van Belkum A, van Wamel WJ. 2011. Immune evasion cluster-
607 positive bacteriophages are highly prevalent among human *Staphylococcus*
608 *aureus* strains, but they are not essential in the first stages of nasal colonization.
609 Clin Microbiol Infect 17:343-8.
610 30. de Haas CJ, Veldkamp KE, Peschel A, Weerkamp F, Van Wamel WJ, Heezius
611 EC, Poppelier MJ, Van Kessel KP, van Strijp JA. 2004. Chemotaxis inhibitory
612 protein of *Staphylococcus aureus*, a bacterial antiinflammatory agent. J Exp Med
613 199:687-95.
614 31. Kwiecinski J, Josefsson E, Mitchell J, Higgins J, Magnusson M, Foster T, Jin T,
615 Bokarewa M. 2010. Activation of plasminogen by staphylokinase reduces the
616 severity of *Staphylococcus aureus* systemic infection. J Infect Dis 202:1041-9.
617 32. Rooijakkers SH, Ruyken M, Roos A, Daha MR, Presanis JS, Sim RB, van Wamel
618 WJ, van Kessel KP, van Strijp JA. 2005. Immune evasion by a staphylococcal
619 complement inhibitor that acts on C3 convertases. Nat Immunol 6:920-7.
620 33. Novick RP. 2003. Autoinduction and signal transduction in the regulation of
621 staphylococcal virulence. Mol Microbiol 48:1429-49.

622 34. Stragier P, Kunkel B, Kroos L, Losick R. 1989. Chromosomal rearrangement
623 generating a composite gene for a developmental transcription factor. Science
624 243:507-12.
625 35. Kunkel B, Losick R, Stragier P. 1990. The *Bacillus subtilis* gene for the
626 development transcription factor sigma K is generated by excision of a
627 dispensable DNA element containing a sporulation recombinase gene. Genes
628 Dev 4:525-35.
629 36. Dubnau D, Losick R. 2006. Bistability in bacteria. Mol Microbiol 61:564-72.
630 37. Veening JW, Smits WK, Kuipers OP. 2008. Bistability, epigenetics, and bet-
631 hedging in bacteria. Annu Rev Microbiol 62:193-210.
632 38. Sambrook J, Fritsch EF, Maniatis T. 1989. Molecular cloning : a laboratory
633 manual, second edition. Cold Spring Harbor Laboratory, Cold Spring Harbor,
634 N. Y.
635 39. Arnaud M, Chastanet A, Debarbouille M. 2004. New vector for efficient allelic
636 replacement in naturally nontransformable, low-GC-content, gram-positive
637 bacteria. Appl Environ Microbiol 70:6887-91.
638 40. Murphy E. 1985. Nucleotide sequence of a spectinomycin adenyltransferase
639 AAD(9) determinant from *Staphylococcus aureus* and its relationship to AAD(3")
640 (9). Mol Gen Genet 200:33-39.
641 41. Steinmetz M, Richter R. 1994. Easy cloning of mini-Tn*10* insertions from the
642 *Bacillus subtilis* chromosome. J Bacteriol 176:1761-3.
643 42. Archambaud C, Gouin E, Pizarro-Cerda J, Cossart P, Dussurget O. 2005.
644 Translation elongation factor EF-Tu is a target for Stp, a serine-threonine
645 phosphatase involved in virulence of *Listeria monocytogenes*. Mol Microbiol
646 56:383-96.
647 43. Livak KJ, Schmittgen TD. 2001. Analysis of relative gene expression data using
648 real-time quantitative PCR and the 2(-Delta Delta C(T)) method. Methods
649 25:402-8.
650 44. Haque RU, Baldwin JN. 1964. Types of hemolysins produced by *Staphylococcus*
651 *aureus*, as determined by the replica plating technique. J Bacteriol 88:1442-7.
652 45. Stokes RW, Doxsee D. 1999. The receptor-mediated uptake, survival, replication,
653 and drug sensitivity of *Mycobacterium tuberculosis* within the macrophage-like
654 cell line THP-1: a comparison with human monocyte-derived macrophages.
655 Cell Immunol 197:1-9.

656 46. Soutourina O, Dubrac S, Poupel O, Msadek T, Martin-Verstraete I. 2010. The
657 pleiotropic CymR regulator of *Staphylococcus aureus* plays an important role in
658 virulence and stress response. PLoS Pathog 6:e1000894.
659

660 **FIGURE LEGENDS**
661
662 **Figure 1: Prophage Φ13 excision in vitro and in vivo.**
663 A) Prophage excision frequencies in strain HG001. qRT-PCR quantification of Φ11, 12,
664 and 13 prophage content in *S. aureus* strain HG001 grown in TSB at 37°C with aeration.
665 Specific primer pairs are described in Supplementary Table 2. The results are the mean
666 of 4 technical replicates and are representative of 3 independent biological replicates.
667 B) Quantification of Φ13 lysogens in bacterial populations from infected kidneys. Mice
668 were infected from the caudal lateral vein with a sub-lethal dose (2 X 10^7 c.f.u.) of *S.*
669 *aureus* strain HG001 Φ13::*aad*(9). Mice were sacrificed four days post-infection and
670 kidneys harvested for c.f.u. counts on TSA and TSA with spectinomycin. 25 infected
671 kidneys were examined and the proportion of homogeneous lysogen population (less
672 than 0.5% non-lysogen) and heterogeneous bacterial population with a mix of lysogen
673 and non-lysogen bacteria is shown.
674 C) Proportion of non-lysogen bacteria per kidney in organs infected with a mixed
675 population of lysogenic and non-lysogenic bacteria.
676
677 **Figure 2: Characterization of the *S. aureus* Δ*int* and ΔΦ13 mutants.** Strains were
678 grown overnight at 37°C with aeration.
679 A) 3 µl of the bacterial cultures was spotted on sheep blood agar plates and incubated
680 consecutively for 24 h at 37°C and 24 h at 4°C to detect hemolytic activities. The white
681 arrow indicates the β-hemolytic halo characteristic of bacteria lacking prophage Φ13.
682 B) Prophage Φ13 excision frequency detected by qRT-PCR using oligonucleotide pairs
683 OMA7-OMA8 and OMA7-OMA9, specific for the presence or absence of Φ13,
684 respectively. A Φ13 lysogen strain was included as a control to confirm the specificity
685 of the amplicons used to quantify Φ13 lysogeny. Results are presented as means ± SEM
686 of 3 replicates and *t*-test was used to compare WT and Δ*int* results (***, p<0,0001).
687
688 **Figure 3: Impact of prophage Φ13 and *hlb* on *S. aureus* virulence.**
689 A) Kaplan-Meier survival curves of *RjOrl:SWISS* mice infected intravenously with
690 *S. aureus* HG001 wild type strain and the Δ*int* and ΔΦ13 mutants (5 X 10^7
691 c.f.u./injection). A total of 14 mice were used in each group in two independent
692 experiments. For each strain, the genotype is indicated followed by the relevant
693 genetic context (presence or absence of prophage Φ13 and a functional *hlb* gene).

694 Statistical analysis of data using Log-rank (Mantel Cox) test was performed to compare
695 each mutant strain to the HG001 parental strain. WT/Δ*int*: *p*=0.0077; WT/ ΔΦ13 :
696 *p*=0.0021.
697 B) Histopathological kidney analyses 6 days post-infection by intravenous inoculation
698 with sub-lethal bacterial loads (2 X 10^7 c.f.u./injection) of the *S. aureus* HG001 wild
699 type (1 and 2), Δ*int* (3 and 4) and ΔΦ13 (5 and 6) strains. Most (5/6) mice infected with
700 the wild type strain displayed mild to moderate nephritis, with neutrophilic
701 infiltrates/abscesses (black arrowheads) of varying sizes in the cortex (1), medulla, and
702 papilla (2). Infection with strain ΔΦ13 led to more severe nephritis (5/6 mice), with
703 multifocal abscesses (3 and 4, black arrowheads), extension to tubules and interstitium,
704 and ischemic necrosis of the papilla (4, black arrow). Most mice (4/6) infected with the
705 Δ*int* strain displayed less severe lesions, with mononuclear cell infiltrates most often
706 in the cortex (5, not seen at a low magnification) but also in the papilla (6, arrowhead).
707
708 **Figure 4: Impact of Φ13 on cytokine induction by THP-1 neutrophils.** PMA-activated
709 THP-1 cells were infected with the HG001 wild type strain or the ΔΦ13 and Δ*int*
710 mutants with a m.o.i. = 10. After 24 H of infection, cytokine gene expression was
711 determined by qRT-PCR performed with cDNA synthesized from RNA of THP-1 cells
712 infected by the indicated strains (dark grey) or non-infected control (light grey).
713 Expression levels are given in arbitrary units normalized against that of HPRT. Each
714 experiment was carried out 6 times in two independent series (means ± SD). ***:
715 *P*<0.005 (*t*-test).
716
717 **Figure 5: Impact of *hlb* on *S. aureus* virulence.** Kaplan-Meier survival curves of
718 *RjOrl:SWISS* mice infected intravenously with *S. aureus* HG001 wild type strain and
719 the Δ*int* hlb_{comp}, ΔΦ13 and ΔΦ13Δ*hlb* mutants (5 X 10^7 c.f.u./injection). A total of 14 mice
720 were used in each group in two independent experiments. *, *P*<0.05 and **, *P*<0.01
721 (Wilcoxon test). For each strain, the genotype is indicated followed by the relevant
722 genetic context (presence or absence of prophage Φ13 and a functional *hlb* gene).
723 A) Role of *hlb* in virulence by comparing infection with the HG001 strain and the ΔΦ13
724 and ΔΦ13Δ*hlb* derivatives. Statistical analysis of data using Log-rank (Mantel Cox) test
725 was performed to compare results from each mutant strain to the HG001 parental
726 strain. WT/ΔΦ13Δ*hlb*: *p*=0.6157 (ns); WT/ΔΦ13 : *p*=0.0039.

727 B) Role of Φ13 in virulence by comparing infection with the HG001 strain and the
728 Δ*int hlb*$_{comp}$ (dashed line) and ΔΦ13 derivatives. Statistical analysis of data using Log-
729 rank (Mantel Cox) test was performed to compare data for mutant strains to the HG001
730 parental strain. WT / Δ*int hlb*$_{comp}$: p=0.0147; WT / ΔΦ13 : p=0.0066.

Figure 1

A.

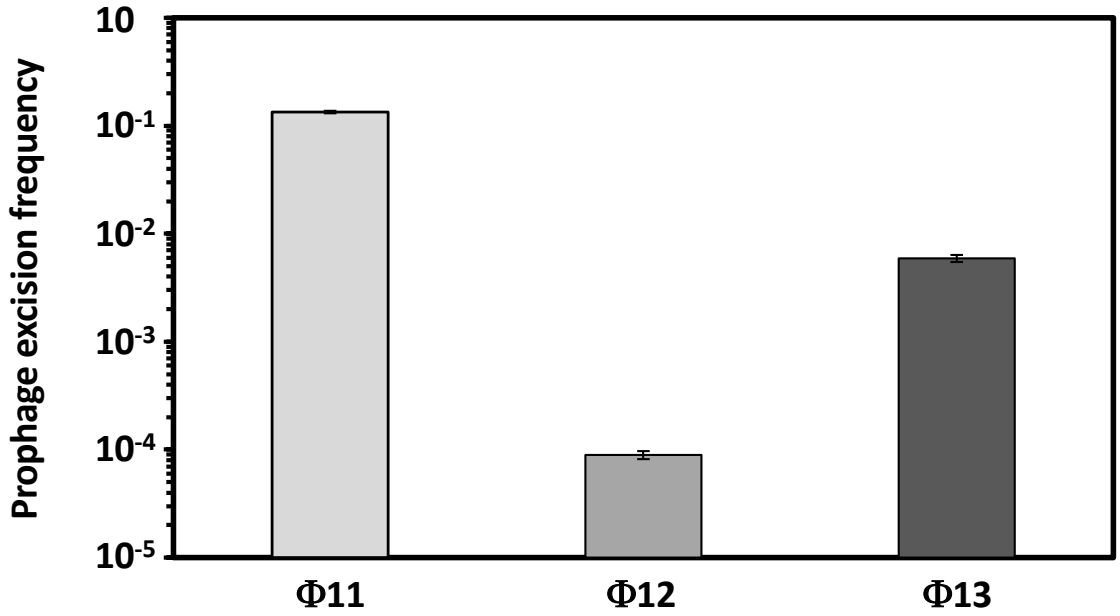
Prophage excision frequency
10
10-1
10-2
10-3
10-4
10-5
Φ11
Φ12
Φ13

B.

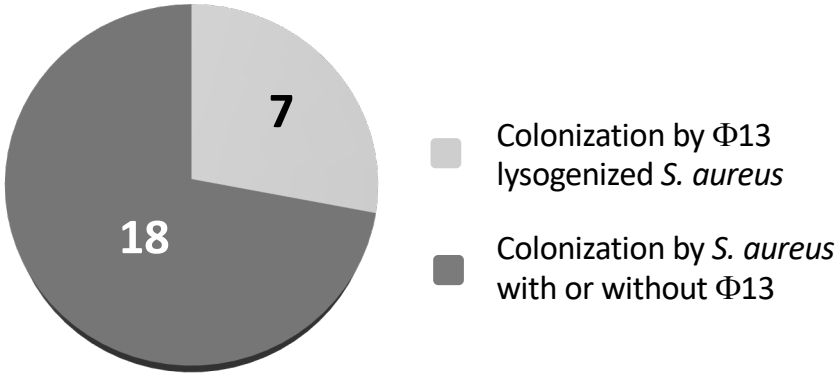
7
18
Colonization by Φ13 lysogenized *S. aureus*
Colonization by *S. aureus* with or without Φ13

C.

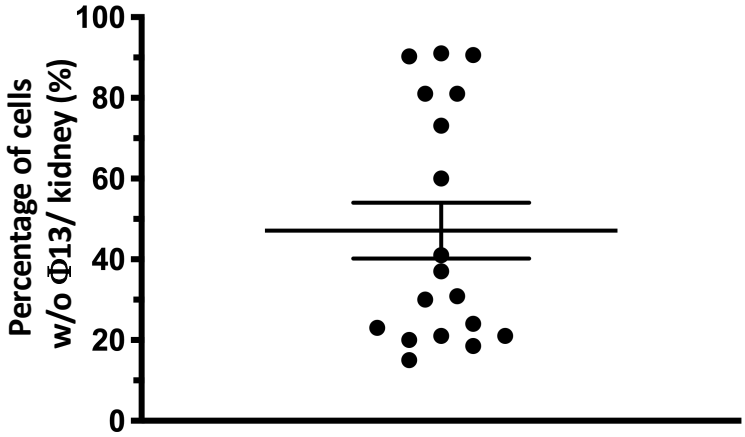
Percentage of cells w/o Φ13/ kidney (%)
100
80
60
40
20
0

Figure 2

A.

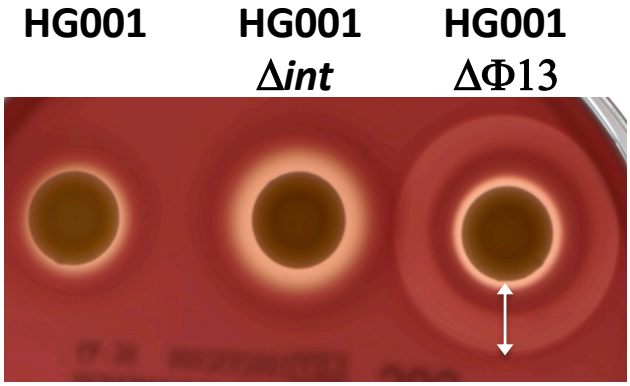
HG001
HG001
Δint
HG001
ΔΦ13

B.

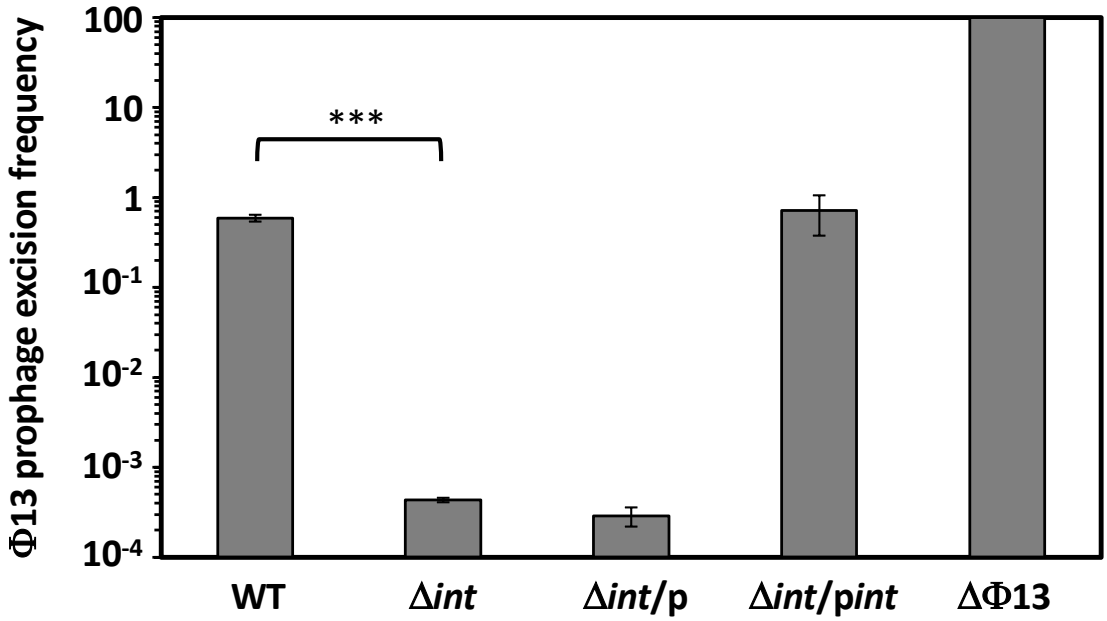
Φ13 prophage excision frequency
100
10
1
10-1
10-2
10-3
10-4
***
WT
Δint
Δint/p
Δint/pint
ΔΦ13

Figure 3

A.

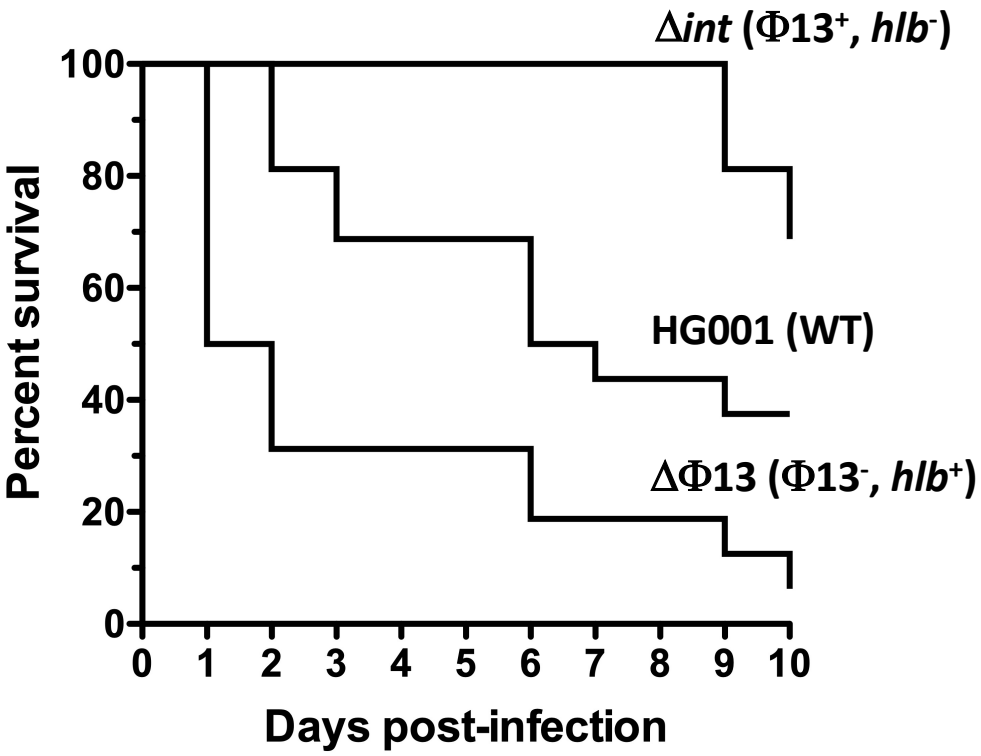
Δint (Φ13+, hlb-)
HG001 (WT)
ΔΦ13 (Φ13-, hlb+)
Percent survival
100
80
60
40
20
0
0 1 2 3 4 5 6 7 8 9 10
Days post-infection

B.

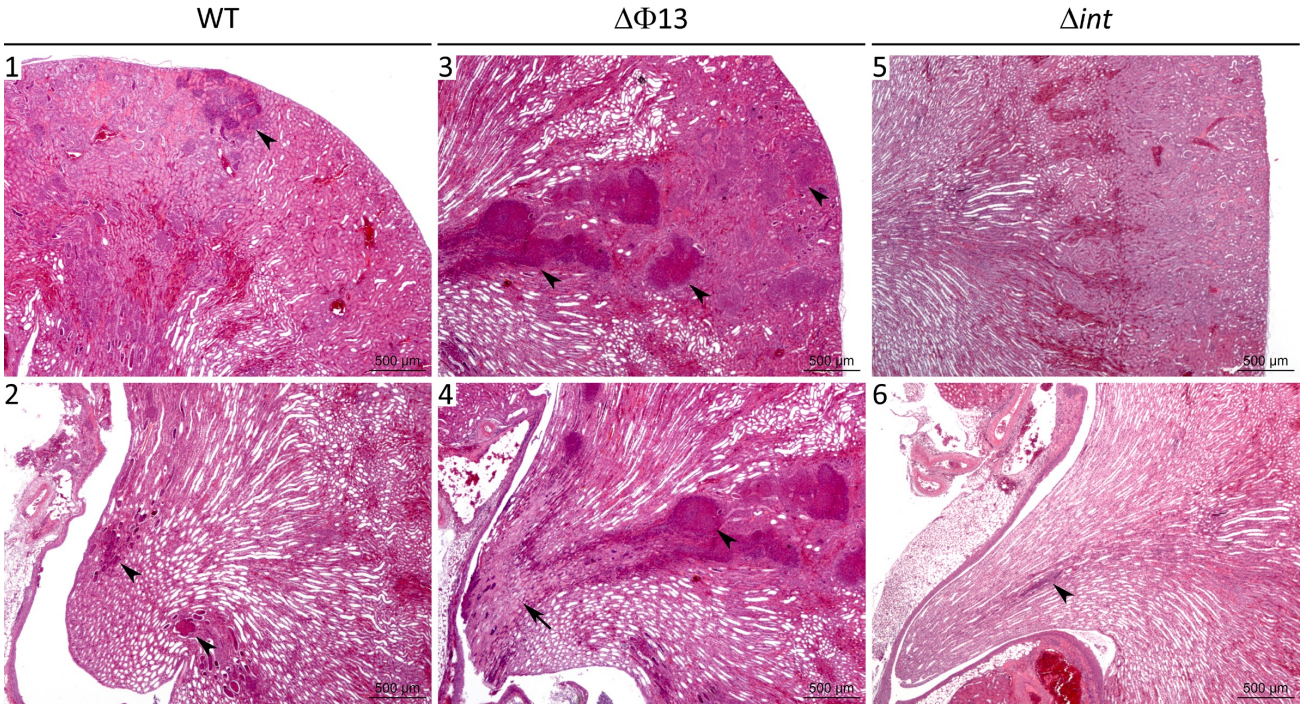
WT
ΔΦ13
Δint
1
2
3
4
5
6
500 µm

Figure 4

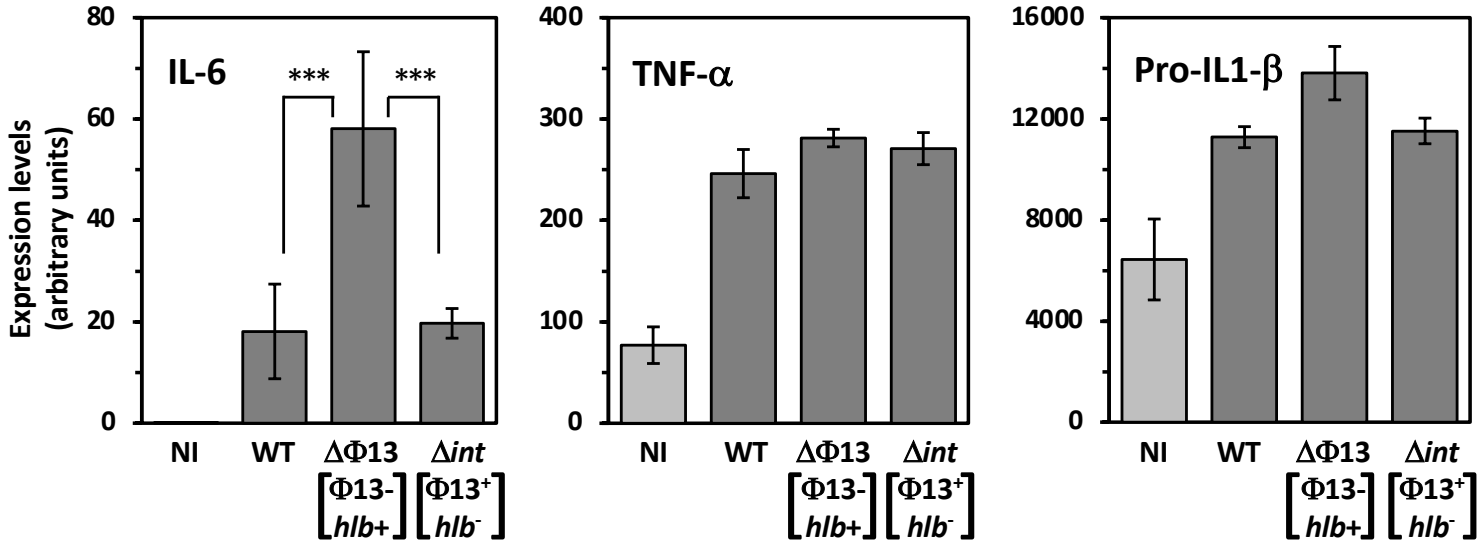
Expression levels (arbitrary units)
IL-6
***
***
80
60
40
20
0
NI
WT
ΔΦ13
Δint
[Φ13- hlb+]
[Φ13+ hlb-]
TNF-α
400
300
200
100
0
Pro-IL1-β
16000
12000
8000
4000

Figure 5

A.

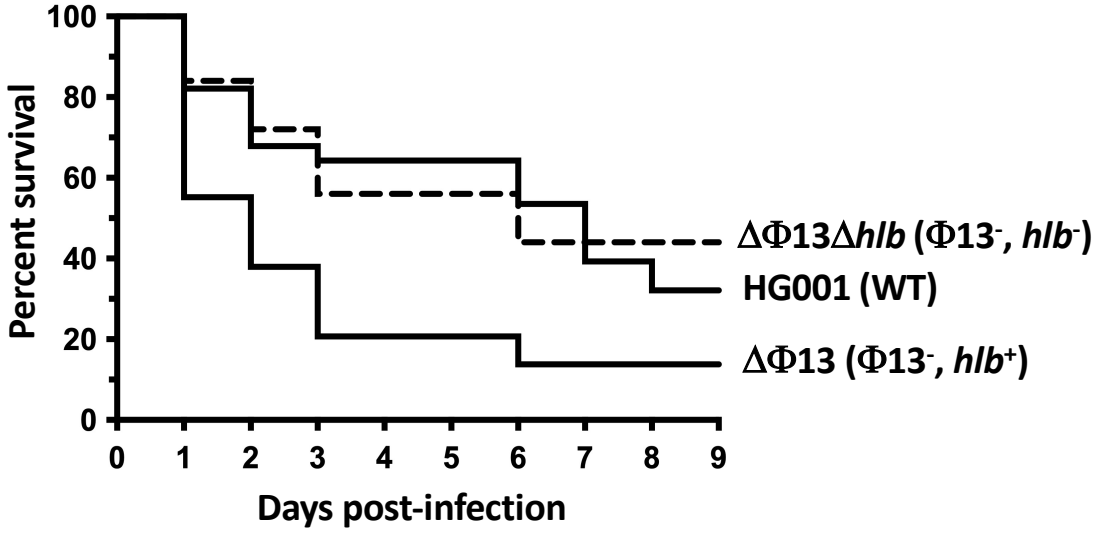
100
80
60
40
20
0
Percent survival
0 1 2 3 4 5 6 7 8 9
Days post-infection
ΔΦ13Δhlb (Φ13-, hlb-)
HG001 (WT)
ΔΦ13 (Φ13-, hlb+)

B.

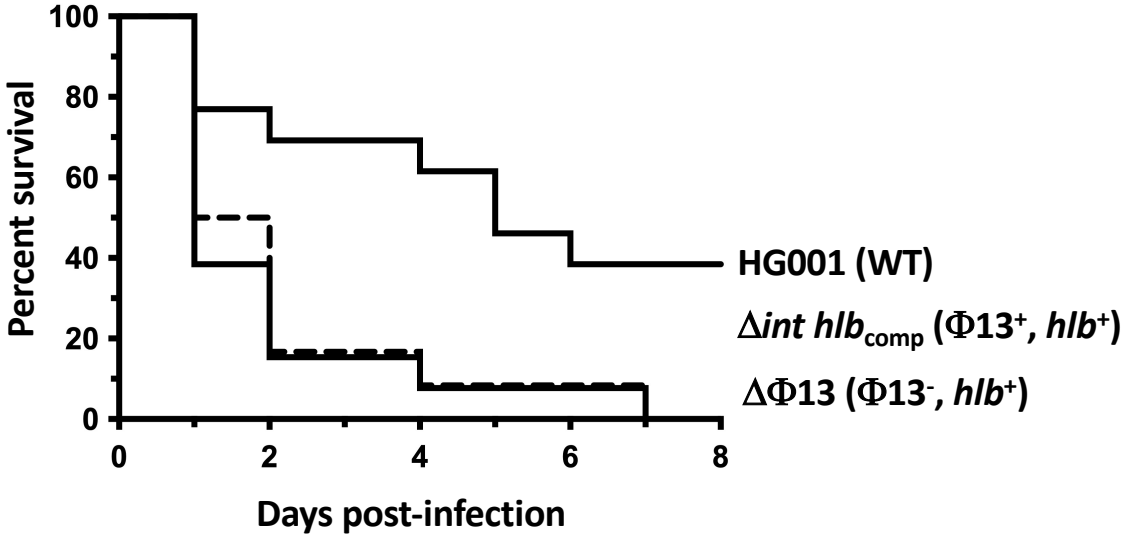
100
80
60
40
20
0
Percent survival
0 2 4 6 8
Days post-infection
HG001 (WT)
Δint hlbcomp (Φ13+, hlb+)
ΔΦ13 (Φ13-, hlb+)

Timely excision of prophage Φ13 is essential for the *Staphylococcus aureus* infectious process

Poupel *et al*. IAI00124-25

Supplementary Information

A.

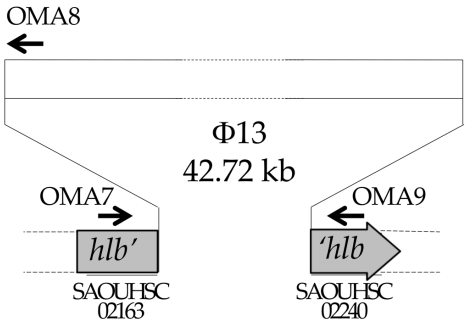

B.

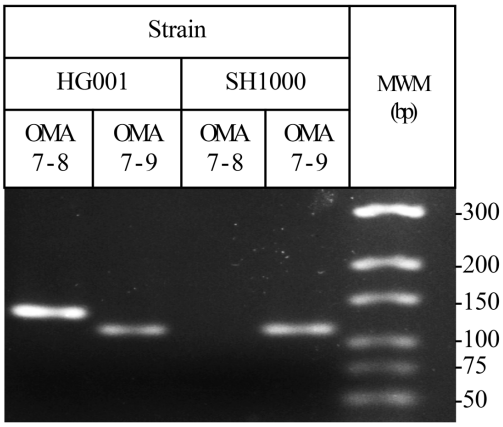

Supplementary Data Fig. 1
PCR-based detection of phage Φ13 insertion and excision

A: The Φ13 chromosomal insertion locus in strain HG001 (not to scale). The Φ13 *att*P sequence is homologous to the *att*B site located within the *hlb* gene encoding β-hemolysin. Φ13 insertion thus results in disruption and inactivation of the *hlb* gene. Specific primers used to quantify the proportion of lysogenic bacteria are indicated, pair OMA7-OMA8 is specific for Φ13 insertion and pair OMA7-OMA9 for the absence of Φ13.
B: Specific amplicons obtained by PCR with the OMA7-8 and OMA7-9 primer pairs using genomic DNA from either the SH1000 strain, cured for Φ13 (114 bp), or from the Φ13 lysogen strain HG001 (132 and 114 bp).

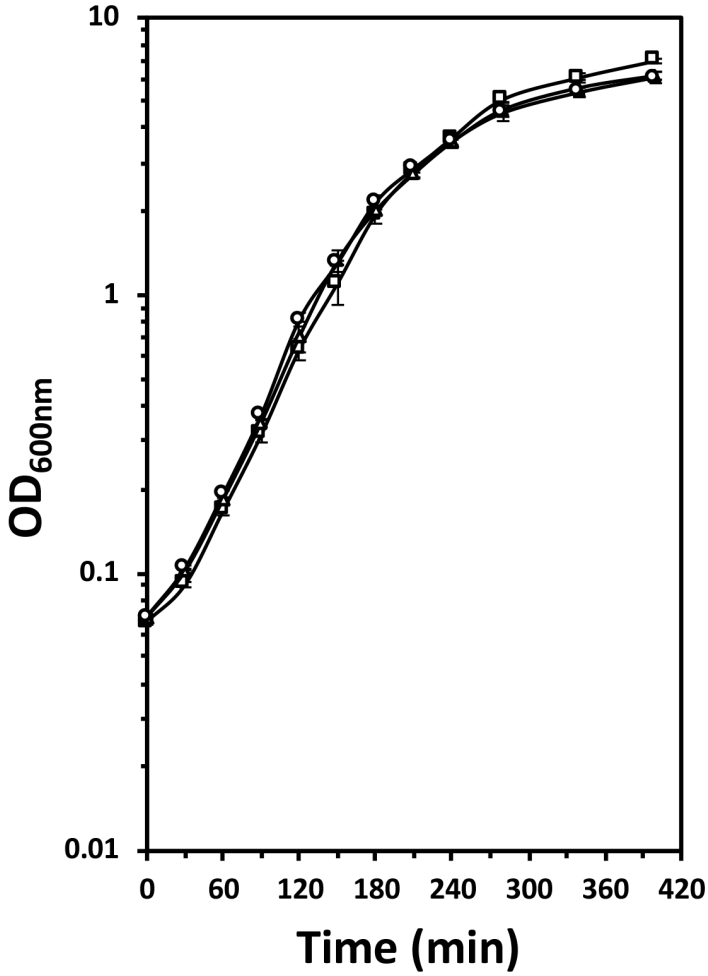

Supplementary Data Fig. 2 Growth curves of *S. aureus* strains HG001 and the ΔΦ13 and Δ*int* mutants.

Bacterial cultures were grown overnight, inoculated in TSB at a calculated OD_{600nm} of 0.05 and incubated at 37°C with aeration. Optical densities were followed over a 6.5 hour period. Results are shown as the mean and standard deviation of three independent growth curves.

Doubling times (http://www.doubling-time.com/compute.php) were calculated during the exponential growth phase (between 60 min and 150 min) and gave values of approximately 32 min for each strain. Strains: HG001 (□); ΔΦ13 (△); Δ*int* (○).

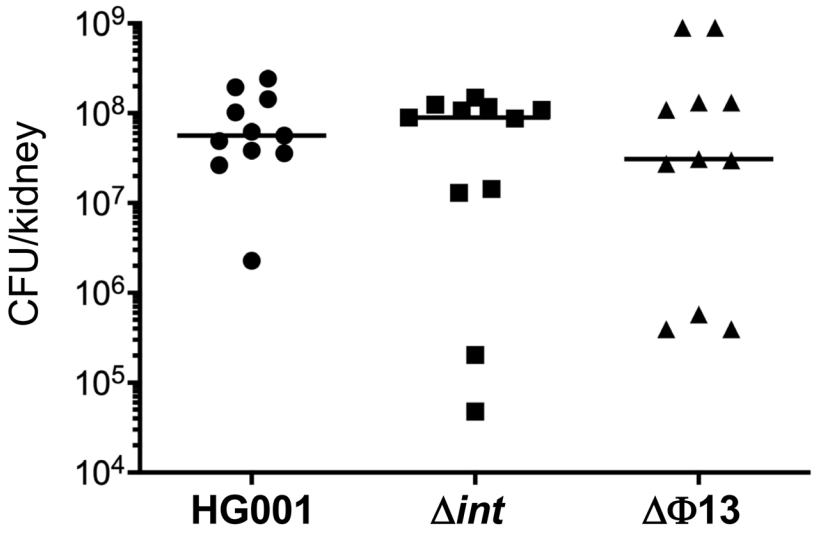

Supplementary Data Fig. 3 Kidney colonization following infection by *S. aureus*
RjOrl:SWISS mice were infected with the *S. aureus* HG001 wild type strain or the Δ*int* and ΔΦ13 derivatives by intravenous injections with a sub-lethal bacterial load (2.10^7 cfu/injection). Six days post-infection, mice were sacrificed, kidneys were harvested and CFU counts carried out. A total of 11 mice were studied in two independent experiments and the data are compilation of the bacterial counts.

A.

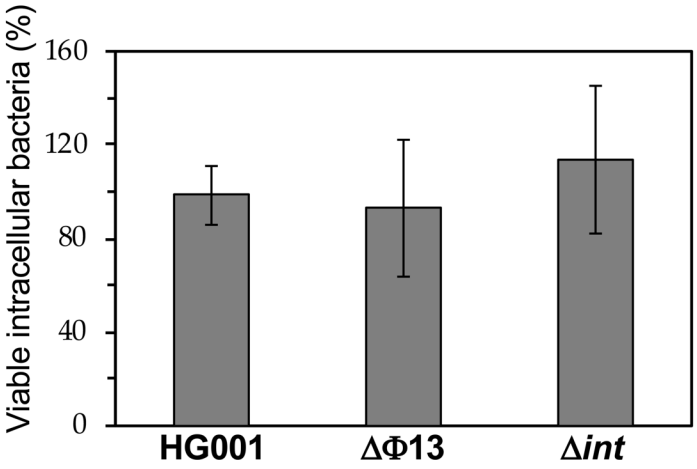

B.

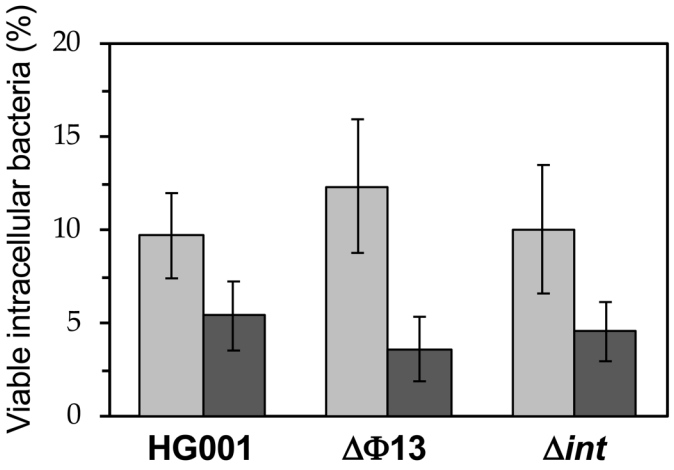

Supplementary Data Fig. 4 Impact of Φ13 on internalization and survival within THP-1 neutrophils.
PMA-activated THP-1 cells were infected with either the HG001 wild type strain or the ΔΦ13 and Δ*int* mutants with a moi=10.
A: Viable intracellular bacteria were quantified two hours post-infection to determine the efficiency of internalization.
B: Viable bacteria were quantified 24 H (light grey) and 48 H (dark grey) post-infection to determine the capacity of each strain to survive within neutrophils.
Results are presented as means and SEM of 3 biological replicates.

Supplementary Data Table 1: Strains and plasmids used in this study

Strain or plasmid	Description	Source or reference
***E. coli* strains**		
DH5α	F⁻ Φ80*lac*ZΔM15 Δ(*lac*ZYA-*arg*F) U169 *rec*A1 *end*A1 *hsd*R17 (r_K–, m_K+) *pho*A *sup*E44 λ– *thi*-1 *gyr*A96 *rel*A1	Invitrogen Life Technology
***S. aureus* strains**		
RN4220	Restriction-deficient transformation recipient strain	[1]
SH1000	NCTC 8325-4 *rsbU*+	[2]
HG001	NCTC 8325 *rsbU*+	[3]
ST1327	HG001Δ*int*	pMAD-*int* → HG001
ST1330	HG001ΔΦ13	pMAD–Φ13 → HG001
ST1346	HG001Δ*int* pMK4P*prot*	pMK4P*prot* → ST1327
ST1347	HG001Δ*int* pMK4P*prot-int*	pMK4P*prot-int* → ST1327
ST1348	HG001Δ*int* Δ*hlb*	pMAD-*hlb* → ST1327
ST1387	HG001Φ13-*aad*(9)	pMAD Φ13-*aad*(9) →HG001
ST1435	HG001Δ*int hlb*comp	pMAD-*hlb*comp → ST1327
Plasmids		
pMAD	Allelic exchange vector	[4]
pMAD–Φ13	pMAD derivative for Φ13 deletion	This study
pMAD-*int*	pMAD derivative for *int* deletion	This study
pMAD-*hlb*	pMAD derivative for *hlb* deletion	This study
pMAD-*hlb*comp	pMAD derivative for *hlb* complementation	This study
pMK4P*prot*	Vector for P*prot*-dependent gene expression (complementation)	[5]
pMK4P*prot-int*	Plasmid used for *int* deletion complementation	This study

1 Kreiswirth, B. N. *et al.* The toxic shock syndrome exotoxin structural gene is not detectably transmitted by a prophage. *Nature* **305**, 709-712, (1983).

2 Horsburgh, M. J. *et al.* σ^B modulates virulence determinant expression and stress resistance: characterization of a functional *rsbU* strain derived from *Staphylococcus aureus* 8325-4. *J. Bacteriol.* **184**, 5457-5467, (2002).

3 Herbert, S. *et al.* Repair of global regulators in *Staphylococcus aureus* 8325 and comparative analysis with other clinical isolates. *Infect. Immun.* **78**, 2877-2889, (2010).

4 Arnaud, M., Chastanet, A. & Debarbouille, M. New vector for efficient allelic replacement in naturally nontransformable, low-GC-content, gram-positive bacteria. *Appl. Environ. Microbiol.* **70**, 6887-6891, (2004).
5 Archambaud, C., Gouin, E., Pizarro-Cerda, J., Cossart, P. & Dussurget, O. Translation elongation factor EF-Tu is a target for Stp, a serine-threonine phosphatase involved in virulence of *Listeria monocytogenes*. *Mol. Microbiol.* **56**, 383-396, (2005).

Supplementary Data Table 2 : Oligonucleotides used in this study

Name	Sequence	Description
Construction of pMAD derivatives		
OSA418	TGGGATCCTAGTCTTAAATCTATATCACTAATACC	Φ13 upstream and downstream fragment (*Bam*HI/*Eco*RI)
OSA419	CAGAATTCAACAATATAACTCGCTTCGTCC	
OSA411	AAAGGATCCTACAAGTGTAGACGTTGAATGGTGGTGAG	*int* upstream fragment (*Bam*HI/*Eco*RI)
OSA412	CGTGAATTCATGCGTTCCCTCCTCAAAATTGGC	
OSA413	AGTGAATTCTTTAGGGACCCATTAGGGACTCCAAACCC	*int* downstream fragment (*Eco*RI/*Nco*I)
OSA414	ATATACATCCCATGGCTTAGGTTTTTCAGTCAC	
OSA442	ATCGGATCCATTGTGTATGGAACTTGGTAATTTGC	*hlb* upstream fragment (*Bam*HI/*sal*I)
OSA443	TTTGTCGACCATTATCACTCCTTTTATATAGCTTAC	
OSA444	TGTGTCGACTGCTCAACTAACTAATAACTTGCTTCG	*hlb* downstream fragment (*Sal*I/*Eco*RI)
OSA445	AATGAATTCAACAATACAAATGTGACTGACTTTGCACC	
OSA508	TTTGGATCCTTACTGACTGCACTTAAATATTATTTAGAC	*aad*(9) insertion upstream fragment (*Bam*HI/*sal*I)
OSA509	GACGTCGACGGAGGATTTTAAATGTTTAAGG	
OSA510	AAACCATGGCTTTCCGTCACTCTTTAATTGG	*aad*(9) insertion downstream fragment (*Nco*I/*Bgl*II)
OSA511	AAGAGATCTTGAAACTTTTTCTCTCATTTAGTGC	
OSA299	ATGTCGACGGATCTTCACCTAGATCCTTTTGAC	*aad*(9) amplicon (*Sal*I/*Nco*I)
OSA470	TTCCCATGGTACAAATTGTTTCACTAAATTAAAGT	
OSA418	TGGGATCCTAGTCTTAAATCTATATCACTAATACC	*hlb* and its upstream region (*Bam*HI/*Sal*I)
OSA573	TCAGTCGACAACAATATAACTCGCTTCGTCC	
OSA574	CCAGTCGACAGACTTTTAACATAAAATTACTTATC	*att*L downstream region of □13 (*Sal*I/*Bgl*II)
OSA575	AAAAGATCTAAGTTTAACCAATATGTTGCTCG	
pMK4Pprot complementation		
OSA446	AACGGATCCCTAAATTTTGGGTAGCCCGCCTACCC	*int* gene amplification (*Bam*HI/*Sal*I)
OSA447	AACGTCGACACAACAGTATTTATTGGGTTTGGAGTCC	
qRT-PCR experiments		
OMA7	GAAAGATGATACTGATTTGA	Amplicon specific for Φ13 presence (OMA7-OMA8) and absence (OMA7-OMA9)
OMA8	AACCTTGATATTATGCTGTT	
OMA9	TAAGAAGATTGTCCGATTA	
OSA438	TACAAACAACTTCAAACTGTTGTGC	
OSA439	AAACATGCGTGGAAAACACAGAGG	

OMA25	CAAATGGGAGCCTTTTCTTA	Amplicon specific for Φ12 presence (OSA438-OSA439) and absence (OSA438-OMA25)
OMA18	AAGGAAGTTTAAGACGATGAA	Amplicon specific for Φ11 presence (OMA18-OMA19) and absence (OMA18-OMA20)
OMA19	AAACGCATTAAATCAACG	
OMA20	TGGCTACAACGCATATTAC	